A LINEAR BARYCENTRIC RATIONAL INTERPOLANT
ON STARLIKE DOMAINS[*]

JEAN-PAUL BERRUT[†] AND GIACOMO ELEFANTE[‡]

Abstract. When an approximant is accurate on an interval, it is only natural to try to extend it to multi-dimensional domains. In the present article we make use of the fact that linear rational barycentric interpolants converge rapidly toward analytic and several-times differentiable functions to interpolate them on two-dimensional starlike domains parametrized in polar coordinates. In the radial direction, we engage interpolants at *conformally shifted Chebyshev nodes*, which converge exponentially for analytic functions. In the circular direction, we deploy linear rational trigonometric barycentric interpolants, which converge similarly rapidly for periodic functions but now for *conformally shifted equispaced nodes*. We introduce a variant of a tensor-product interpolant of the above two schemes and prove that it converges exponentially for two-dimensional analytic functions—up to a logarithmic factor—and with an order limited only by the order of differentiability for real functions (provided that the boundary enjoys the same order of differentiability). Numerical examples confirm that the shifts permit one to reach a much higher accuracy with significantly fewer nodes, a property which is especially important in several dimensions.

Key words. barycentric rational interpolation, trigonometric interpolation, Lebesgue constant, conformal maps, starlike domains

AMS subject classifications. 41A10, 42A15, 41A20, 65D05

1. Introduction. Interpolating a function in several dimensions is a fundamental research topic in applied mathematics due to its many applications in engineering and many other fields; one must only recall finite element and pseudospectral methods for partial differential equations. In the present work, we shall merely be interested in infinitely smooth interpolants. For the abundant literature on splines, the reader may consult [27], among the many books on the subject.

Classical multivariate rational interpolation has been widely studied [1, 15]. As in the uni-dimensional case, it has the ability to better deal with singularities of the function than polynomials [18]. Unfortunately, rational approximation can be numerically fragile to compute, and it is inclined to spurious singularities. Many different approaches have been introduced to avoid these drawbacks, such as algorithms based on the singular value decomposition [28] or on a Stieltjes procedure and an optimization formulation [2].

In this work we aim to construct smooth surfaces by interpolating over non-trivial two-dimensional domains, e.g., domains that are neither rectangles nor disks. Since the number of interpolation points grows very rapidly in several dimensions ("curse of dimensionality"), we want to use fast converging approximants such as the polynomial interpolant at Chebyshev points. However, even the latter is inaccurate for functions with large gradients, as documented in the first line of each of the tables in [12]. Put in another way, a large number of nodes in every direction (quickly more than 1000) is necessary for an accurate approximation, which is difficult in several dimensions on a classical personal computer.

It has been known for a long time that in such situations one should concentrate the nodes in the vicinity of large gradients (in the context of the solution of time evolution PDEs one speaks of moving meshes). To maintain the rapid convergence of the infinitely smooth interpolant, one uses for that purpose infinitely differentiable or even analytic point shifts [5].

[†]Department of Mathematics, Université de Fribourg, Fribourg, Switzerland (jean-paul.berrut@unifr.ch).
[‡]Department of Mathematics "Tullio Levi-Civita", Università di Padova, Padova, Italy (giacomo.elefante@unipd.it).

Such shifts may be performed in (at least) two ways [8]. One is to change the variable before using the interpolating polynomial; however, the inner derivatives involved in the chain rule rapidly complicate the formulas when the order of derivation increases. Here we shall rather use linear rational barycentric interpolation, whose derivatives may be derived from simple formulas discovered by Schneider and Werner [26] and retain the barycentric nature of the interpolant. The effect of the point shifts on the accuracy is spectacular (compare the fifth line with the first in the tables of [12]).

For simplicity and cheapness, the method we suggest works with a representation of the domain in polar coordinates and is therefore limited to starlike domains. It transplants the problem to a disk and basically consists in a tensor product of a linear rational barycentric interpolant at conformally shifted Chebyshev nodes on the segments in the radial direction with a linear rational trigonometric barycentric interpolant at conformally shifted equispaced nodes in the circular direction.

To retain the rapid convergence of the one-dimensional interpolants, one should obtain these when inserting a constant value of the other variable: for instance, when the radial variable is constant, one should obtain a trigonometric barycentric one-dimensional interpolant in the circular variable. To guarantee this in a simple and cheap way, we represent the domain through a homothety of its boundary, i.e., by multiplying the polar representation of the latter by all numbers between 0 and 1 and the interpolation points by the intersections of such curves with the radii from the origin. The concentration of nodes at locations of large gradients is obtained by concentrating the homothetic curves as well as the radii in the vicinity of such locations.

In the next section, we review the one-dimensional linear rational barycentric interpolants which make up the basis of the suggested method, together with the corresponding convergence results (high-degree algebraic convergence for several-times differentiable functions and exponential convergence for analytic ones). Section 2 recalls the tensor-product interpolation of (linear) rational barycentric interpolants on disks, describes the special case of the interpolants used in our method, and studies the Lebesgue constant of the resulting two-dimensional interpolant, which is interesting for its own sake and as an important ingredient of the convergence theorems of the final scheme. Section 3 introduces the formula for the interpolant at shifted nodes on starlike domains and studies its Lebesgue constant, which arises in the error estimates of Section 4. Section 5 demonstrates the efficiency of the method by numerical examples. The paper concludes with some general remarks on the scheme.

2. Preliminaries. Let us consider $n + 1$ distinct nodes in $[a, b]$, which we denote by x_i, $i = 0, \ldots, n$, with their corresponding data f_i. In case we interpolate a function f, we define the f_i as $f_i := f(x_i)$. Then, it is well known (see, e.g., [20, p. 238]) that the unique polynomial of degree at most n interpolating the f_i may be written in the barycentric form

$$p_n(x) = \frac{\sum_{i=0}^{n} \frac{\lambda_i}{x - x_i} f_i}{\sum_{i=0}^{n} \frac{\lambda_i}{x - x_i}},$$

with the so-called weights λ_i defined by

$$\lambda_i = \prod_{\substack{j=0 \\ j \neq i}}^{n} \frac{1}{x_i - x_j}.$$

In case the nodes are the Chebyshev points of the second kind, i.e.,

$$x_i = -\cos\left(\frac{i\pi}{n}\right), \qquad i = 0, \ldots, n,$$

the weights are (up to a constant) [20, p. 252]

$$\lambda_i = (-1)^i \delta_i, \tag{2.1}$$

with δ_i equal to $1/2$ for the first and the last nodes and equal to 1 for the others. The interpolant therefore becomes

$$p_n(x) = \frac{\sum_{i=0}^{n} {}'' \frac{(-1)^i}{x-x_i} f_i}{\sum_{i=0}^{n} {}'' \frac{(-1)^i}{x-x_i}}, \tag{2.2}$$

where the double prime means that the first and the last terms of the sum are halved.

With these nodes, p_n enjoys excellent convergence properties when the interpolated function is smooth (see, e.g., [29, p. 53]). Throughout this article, an unadorned $\|\cdot\|$ denotes the infinity norm.

THEOREM 2.1. *Let $\nu \geq 1$ be an integer, and let f and its derivatives up to $f^{(\nu-1)}$ be absolutely continuous on $[-1,1]$ and the νth-derivative be of bounded variation with V its total variation. Then, for any $n \geq \nu$, the Chebyshev interpolant satisfies*

$$\|f - p_n\| \leq \frac{4V}{\pi\nu(n-\nu)^\nu}.$$

For functions that are not just smooth but *analytic* on $[-1,1]$, the rate of convergence is geometric ([25, p. 143]). An analytic function on $[-1,1]$ is actually analytic in a *Bernstein ellipse E_σ*, which is the region of $\mathbb{C}$ bounded by the ellipse with foci at ± 1 and sum of the lengths of the semiminor and the semimajor axes equal to $\sigma > 1$. For functions analytic in E_σ we have:

THEOREM 2.2. *Let f be a function analytic inside and on an ellipse E_σ. Then, for each $n \geq 0$, the polynomial interpolant between Chebyshev points of the first or the second kind satisfies*

$$\|f - p_n\| \leq \frac{4M}{\sigma^n(\sigma-1)},$$

where $M = \max_{z \in E_\sigma} |f(z)|$.

For other nodes than Chebyshev points, the expression (2.2) becomes a linear rational interpolant [6]. Baltensperger et al. proved in [4] that exponential convergence then still holds for Chebyshev nodes shifted with a conformal map, say g. In fact, in this case we have the following theorem for the interpolant

$$r_n(x) = \frac{\sum_{i=0}^{n} {}'' \frac{(-1)^i}{g(x)-g(x_i)} f(g(x_i))}{\sum_{i=0}^{n} {}'' \frac{(-1)^i}{g(x)-g(x_i)}}. \tag{2.3}$$

THEOREM 2.3. *Let $\mathcal{D}_1$, $\mathcal{D}_2$ be two domains of $\mathbb{C}$ containing $J = [-1,1]$, respectively $I(\subset \mathbb{R})$, let g be a conformal map $\mathcal{D}_1 \to \mathcal{D}_2$ such that $g(J) = I$, and let f be a function $\mathcal{D}_2 \to \mathbb{C}$ such that the composition $f \circ g : \mathcal{D}_1 \to \mathbb{C}$ is analytic inside and on an ellipse E_σ $(\subset \mathcal{D}_1)$, $\sigma > 1$, with foci -1 and 1 and with the sum of the semiminor and the semimajor axes equal to σ. Let r_n be the interpolant (2.3) interpolating f at the transformed Chebyshev nodes $y_i = g(x_i)$, $i = 0, \ldots, n$. Then,*

$$\|f - r_n\| = \mathcal{O}(\sigma^{-n}).$$

Note that, if we write $y = g(x)$ and $y_i = g(x_i)$, for $i = 0, \ldots, n$, then r_n can be represented as

$$\tilde{r}_n(y) = \frac{\sum_{i=0}^{n} {}'' \frac{(-1)^i}{y-y_i} f(y_i)}{\sum_{i=0}^{n} {}'' \frac{(-1)^i}{y-y_i}},$$

which corresponds to Berrut's second interpolant [21] R_1, introduced in [6], at the nodes y_i.

We now turn to periodic interpolants. For the equidistant nodes

$$(2.4) \qquad\qquad \theta_i = i \cdot \frac{2\pi}{n}, \qquad \text{for } i = 0, \ldots, n-1,$$

in $[0, 2\pi)$, there exists a unique balanced trigonometric polynomial that interpolates the data f_i, $i = 0, \ldots, n-1$, at the nodes, and it can be written in the simple barycentric form

$$(2.5) \qquad\qquad T_n(\theta) = \frac{\sum_{i=0}^{n-1} (-1)^i \operatorname{cst}\left(\frac{\theta - \theta_i}{2}\right) f_i}{\sum_{i=0}^{n-1} (-1)^i \operatorname{cst}\left(\frac{\theta - \theta_i}{2}\right)},$$

where the function cst is

$$\operatorname{cst}(\theta) := \begin{cases} \csc(\theta), & \text{if } n \text{ is odd}, \\ \operatorname{ctg}(\theta), & \text{if } n \text{ is even}. \end{cases}$$

Let us define Π as the class of periodic complex-valued functions on $\mathbb{R}$ with period 2π. Then, it is possible to prove convergence theorems for T_n which depend on the smoothness of the function f, as for Chebyshev interpolation (see [20, p. 365] and [30] for the first theorem and [19] for the second).

THEOREM 2.4. *Let $f \in \Pi$ be such that it has at most simple jump discontinuities in the μth-derivative, which is of bounded variation V. Then,*

$$|f(\theta) - T_n(\theta)| \leq \frac{V}{\pi m^\mu} \left(\frac{1}{m} + \frac{2}{\mu}\right),$$

with $m := \lfloor n/2 \rfloor$.

THEOREM 2.5. *Let $f \in \Pi$ be analytic in the strip $S_a := \{\eta : |\operatorname{Im}(\eta)| \leq a\}$, where $a > 0$, and $|f(\theta)| \leq M$. Then,*

$$|f(\theta) - T_n(\theta)| \leq 2M \cot\left(\frac{a}{2}\right) e^{-an}.$$

The first author proposed in [6] to use T_n for nodes other than equidistant points. Then (2.5) becomes a linear rational trigonometric interpolant, which we denote by $t_n \equiv t_n[f]$.

In the wake of the barycentric rational interpolant at the Chebyshev nodes, Baltensperger [3] showed in 2002 that, if we consider as nodes some conformally shifted equidistant points, then the interpolant between these shifted nodes retains the convergence behaviour of the one at the equidistant nodes. In fact the following holds:

THEOREM 2.6. *Let $g \in \Pi$ be a conformal map such that $g(I) = I$ with $I = [0, 2\pi]$ and such that the function*

$$w(\phi, \theta) := \frac{\operatorname{cst}\left(\frac{g(\phi) - g(\theta)}{2}\right)}{\operatorname{cst}\left(\frac{\phi - \theta}{2}\right)}$$

is bounded and analytic in $S_{a_1} \times S_{a_1}$ for an $a_1 > 0$. Let f be a function such that $f \circ g \in \Pi$. Let

$$t_n(\phi) \equiv t_n[f \circ g](\theta) = \frac{\sum_{i=0}^{n-1}(-1)^i \operatorname{cst}\left(\frac{g(\theta)-g(\theta_i)}{2}\right)f(g(\theta_i))}{\sum_{i=0}^{n-1}(-1)^i \operatorname{cst}\left(\frac{g(\theta)-g(\theta_i)}{2}\right)}$$

be the rational function generalizing (2.5) between the nodes $\phi_i := g(\theta_i)$, $i = 0, \ldots, n-1$, where the θ_i are the equidistant nodes (2.4). Then, for every $\phi \in I$, we have the following:

- *If $f \circ g$ has simple jump discontinuities in the μth-derivative, then*

$$|f(\phi) - t_n(\phi)| = \mathcal{O}(n^{-\mu}).$$

- *If $f \circ g$ is analytic in a strip S_{a_2}, with $a_2 \geq a_1 > 0$, and f is bounded, then*

$$|f(\phi) - t_n(\phi)| = \mathcal{O}(\sigma^{-n}) \qquad \text{with } \sigma := e^{a_2}.$$

3. The tensor-product interpolant and its Lebesgue constant. Let the fixed integer $d \geq 2$ be the dimension of the domain of the functions to be interpolated. Then, for each $\ell = 1, \ldots d$, consider a set of interpolating functions $\{b_i^{(\ell)}(x)\}$ over $n_\ell + 1$ nodes x_i in an interval I_ℓ such that

$$b_i^{(\ell)}(x_k) = \delta_{i,k},$$

and form the one-dimensional linear interpolant

$$\mathcal{I}_{n_\ell}^\ell f(x) = \sum_{i=0}^{n_\ell} f(x_i) b_i^{(\ell)}(x).$$

To construct a d-dimensional tensor-product interpolation operator of a multivariate function

$$f := f(\xi_1, \ldots, \xi_d), \qquad f : I^d \to \mathbb{R},$$

in the box $I^d = I_1 \times \cdots \times I_d$, we consider the operator

$$\mathcal{I} : \mathcal{C}(I^d) \to \mathcal{C}(I^d), \qquad \mathcal{I} = \mathcal{I}_{n_1}^1 \otimes \cdots \otimes \mathcal{I}_{n_d}^d,$$

where $\mathcal{I}_{n_l}^l$ is a one-dimensional linear interpolation operator at a set of nodes $x_i^{(\ell)} \in I_\ell$, with $i = 0, \ldots n_\ell$. Then, the tensor-product interpolant is of the form (see, e.g., [22, p. 30])

$$(\mathcal{I}f)(\xi_1, \ldots, \xi_d) = \sum_{i_1=0}^{n_1} \cdots \sum_{i_d=0}^{n_d} f(x_{i_1}^{(1)}, \ldots, x_{i_d}^{(d)}) b_{i_1}^{(1)}(\xi_1) \cdots b_{i_d}^{(d)}(\xi_d).$$

We will now focus on the case $d = 2$ and on the domain

$$B = [0, 2] \times [0, 2\pi).$$

Starting with the first interval, we let $\mathcal{X}_n = \{x_0, \ldots, x_n\}$ be the set of distinct nodes in $[0, 2]$, and we use the basis functions

$$b_i^{(1)}(x) = \frac{\frac{(-1)^i \delta_i \eta_i}{x - x_i}}{\sum_{j=0}^{n_1} \frac{(-1)^j \delta_j \eta_j}{x - x_j}},$$

<div align="center">(a)   (b)</div>
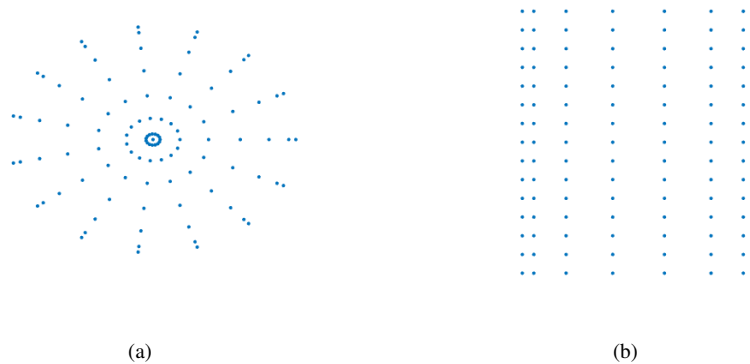
FIG. 3.1. *An example of a grid with $n_1 = 7$ and $n_2 = 15$ in the disk and in the rectangle B.*

in the radial direction, where δ_i is as (2.1) and η_i is defined by

$$\eta_i := \begin{cases} \sqrt{1-(x_i-1)^2}, & 0,2 \notin \mathcal{X}_n, \\ \sqrt{\frac{1+(x_i-1)^2}{2}}, & 0 \notin \mathcal{X}_n, 2 \in \mathcal{X}_n, \\ \sqrt{\frac{1-(x_i-1)^2}{2}}, & 0 \in \mathcal{X}_n, 2 \notin \mathcal{X}_n, \\ 1, & 0,2 \in \mathcal{X}_n. \end{cases}$$

$(b_i^{(1)}(x)$ is the transplantation of $b_i^{(2)}(\phi)$, defined below, to the interval $[0,1]$ through the change of variable $\phi = \arccos x$; the formula for η_i is on $[0,2]$ that of the weights of the polynomial interpolating at the four kinds of Chebyshev points in this interval; see [6]. In the angular direction, we take n_2 distinct nodes $\phi_0, \ldots, \phi_{n_2-1} \in [0, 2\pi)$, and we consider the periodic basis

$$b_i^{(2)}(\phi) = \frac{(-1)^i \operatorname{cst}\left(\frac{\phi-\phi_i}{2}\right)}{\sum_{j=0}^{n_2-1}(-1)^j \operatorname{cst}\left(\frac{\phi-\phi_j}{2}\right)}.$$

On two-dimensional domains this leads to the tensor product

$$\mathcal{I} = R_1 \otimes t_n$$

of Berrut's second interpolant R_1 and the trigonometric interpolant t_n introduced in [6], and it is an operator from the space of continuous functions in B to $\mathcal{R}_n \otimes \mathbf{\Sigma}_n$, where $\mathcal{R}_n$ is the space of rational interpolants of degree n with the same denominator $\sum_{j=0}^n (-1)^j \delta_j \eta_j/(x-x_j)$ and $\mathbf{\Sigma}_n$ is the space of rational trigonometric interpolants of degree $\lfloor \frac{n}{2} \rfloor$ with the same denominator $\sum_{j=0}^{n-1}(-1)^j \operatorname{cst}\left(\frac{\phi-\phi_j}{2}\right)$.

Note that, since the $b_i^{(2)}$ are periodic, this interpolant can be regarded as one in polar coordinates in the disk

(3.1) $$E = \{x \in \mathbb{R}^2 : \|x\|_2 \leq 2\}.$$

To take advantage of the rapid uni-dimensional convergence and the good conditioning of

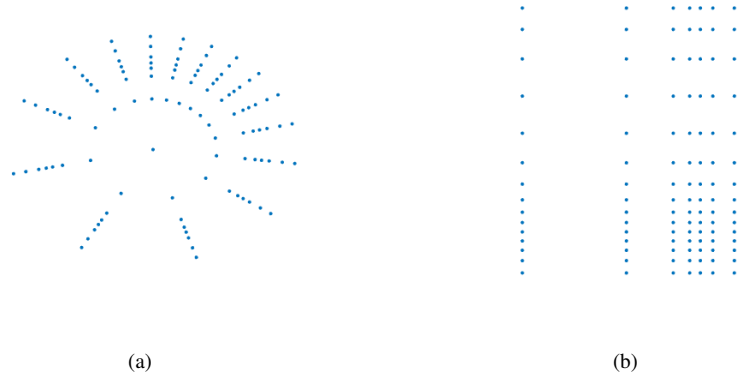(a)   (b)

FIG. 3.2. *An example of a grid with shifted nodes clustered around* $(0.75, \pi/3)$ *in the circle and the rectangle B by using the Bayliss-Turkel map for r and the map introduced in [10] for θ and with* $n_1 = 7$ *and* $n_2 = 15$.

those interpolants, we will consider as nodes the direct product of Chebyshev points of the second kind in $[0, 2]$,

$$r_i = -\cos\left(\frac{i\,\pi}{n_1}\right) + 1, \qquad i = 0, \ldots, n_1,$$

and the equidistant nodes in $[0, 2\pi)$,

$$\theta_j = j \cdot \frac{2\,\pi}{n_2}, \qquad j = 0 \ldots, n_2 - 1.$$

An example of such a direct product is shown in Figure 3.1. Then, the interpolant will be of the form

$$(3.2) \qquad \mathcal{I}[f](r, \theta) = \frac{\sum_{i=0}^{n_1} {}'' \sum_{j=0}^{n_2-1} \frac{(-1)^{i+j}}{r-r_i} \operatorname{cst}\left(\frac{\theta-\theta_j}{2}\right) f(r_i, \theta_j)}{\sum_{i=0}^{n_1} {}'' \sum_{j=0}^{n_2-1} \frac{(-1)^{i+j}}{r-r_i} \operatorname{cst}\left(\frac{\theta-\theta_j}{2}\right)}.$$

Note that using these bases allows us to consider conformally shifted nodes in the two variables and thus the interpolant

$$(3.3) \qquad \mathcal{I}[f](r, \theta) = \frac{\sum_{i=0}^{n_1} {}'' \sum_{j=0}^{n_2-1} \frac{(-1)^{i+j}}{g_1(r)-g_1(r_i)} \operatorname{cst}\left(\frac{g_2(\theta)-g_2(\theta_j)}{2}\right) f(g_1(r_i), g_2(\theta_j))}{\sum_{i=0}^{n_1} {}'' \sum_{j=0}^{n_2-1} \frac{(-1)^{i+j}}{g_1(r)-g_1(r_i)} \operatorname{cst}\left(\frac{g_2(\theta)-g_2(\theta_j)}{2}\right)}$$

with the two uni-dimensional conformal maps

$$g_1 : [0, 2] \to [0, 2] \quad \text{and} \quad g_2 : [0, 2\pi) \to [0, 2\pi).$$

This will allow us to cluster the nodes near a given location $(\bar{r}, \bar{\theta})$, for example by using the Bayliss-Turkel map [5] as g_1 and the map introduced by the authors in [10] as g_2; see Figure 3.2 for an example.

Then, considering the interpolant $\mathcal{I}$ over a grid of $(n_1 + 1)n_2$ nodes in $[0, 2] \times [0, 2\pi)$, we can order the basis functions from $(0, 0)$ to $(n_1, n_2 - 1)$ according to

$$(0,0) \to 0, \quad (0,1) \to 1, \quad (0,2) \to 2, \quad \ldots, \quad (n_1, n_2 - 1) \to n_1(n_2 - 1)$$

and write the interpolant (3.2) in the linear form

$$\mathcal{I}f(r,\theta) = \sum_{j=0}^{n_1(n_2-1)} B_{i_j}(r,\theta)f(r_{i_j},\theta_{i_j}),$$

where

$$B_{i_j}(r,\theta) = b_{i_j}^{(1)}(r)b_{i_j}^{(2)}(\theta)$$

are the basis functions of the interpolant, i.e., $B_{i,j}(r,\theta)$ is equal a 1 in the nodes (r_i,θ_j) and vanishes in the other nodes. The Lebesgue constant of $\mathcal{I}$ is [24, p. 24]

$$\Lambda_{n_1 n_2} = \max_{(r,\theta)\in[0,2]\times[0,2\pi)} \sum_{i_j=0}^{n_1(n_2-1)} |B_{i_j}(r,\theta)|,$$

which is equivalent to

$$\Lambda_{n_1 n_2} = \max_{(r,\theta)\in[0,2]\times[0,2\pi]} \sum_{i=0}^{n_1}\sum_{j=0}^{n_2-1} |b_i^{(1)}(r)| \cdot |b_j^{(2)}(\theta)|$$

$$= \left(\max_{r\in[0,2]} \sum_{i=0}^{n_1} |b_i^{(1)}(r)|\right)\left(\max_{\theta\in[0,2\pi]} \sum_{i=0}^{n_2-1} |b_i^{(2)}(\theta)|\right) = \Lambda_{n_1}^{(1)}\Lambda_{n_2}^{(2)},$$

where $\Lambda_{n_1}^{(1)}$ is the Lebesgue constant of the interpolant R_1 for the $n_1 + 1$ nodes r_i, and $\Lambda_{n_2}^{(2)}$ is that of t_n for the n_2 nodes θ_j and with the second equality valid since the variables are separate and the maximum is in a rectangle.

Since it is proven in [7] that $\Lambda_{n_1}^{(1)} = \mathcal{O}(\log(n_1))$ and in [11] that $\Lambda_{n_2}^{(2)} = \mathcal{O}(\log(n_2))$, this shows the following:

THEOREM 3.1. *The Lebesgue constant of the interpolant* (3.2) *at* $n_1 + 1$ *Chebyshev nodes times* n_2 *equispaced nodes as well as that of the interpolant* (3.3) *at conformally shifted nodes obey*

$$\Lambda_{n_1 n_2} = \mathcal{O}(\log n_1 \log n_2).$$

4. Interpolation on two-dimensional starlike domains. We shall now consider functions on starlike domains [14, p. 92].

DEFINITION 4.1. *A domain* $\Omega \subset \mathbb{R}^2$ *is called* starlike *with respect to a point* $x \in \Omega$ *if for every point* $y \in \Omega$ *the closed segment* $[x,y]$ *is contained in* Ω. *Furthermore, a domain* $\Omega \subset \mathbb{R}^2$ *is called* starlike, *if it is starlike with respect to at least one of its points.*

We shall describe Ω in polar coordinates with $(0,0)$ the center of the domain, i.e., as the domain contained in the curve

$$z(\theta) := \Big(\rho(\theta)\cos(\theta), \rho(\theta)\sin(\theta)\Big)$$

for a 2π-periodic function

$$\rho(\theta) : [0,2\pi] \to \mathbb{R}^{>0},$$

i.e.,

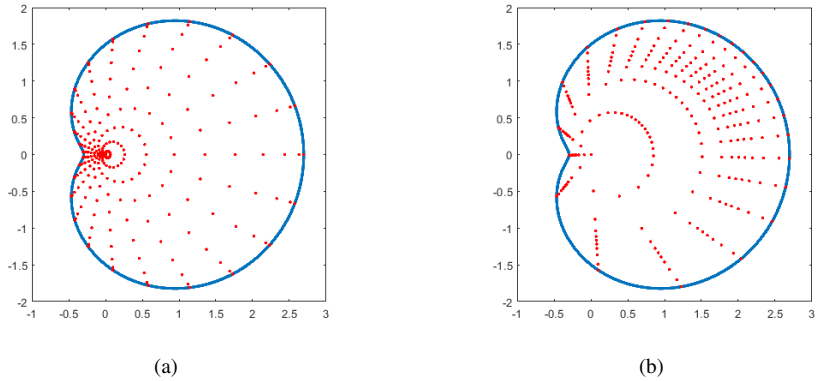$$\Omega := \Big\{(r,\theta) \in \mathbb{R}^2 : r < \rho(\theta)\Big\}.$$

(a)

(b)

FIG. 4.1. *On the left, an example of a mapped uniform grid, and on the right, an example of a mapped conformally shifted grid.*

Our goal is to approximate a function f on $\bar{\Omega}$ by using the interpolant $\mathcal{I}$ of the former section. To that end, we consider the homothetic grid of points in $\bar{\Omega}$, which consists in the grid (see the example in Figure 4.1)

$$G_{i,j} = \Big(r_i \rho(\theta_j), \theta_j \Big) := \Big(\xi_{i,j}, \phi_j \Big) \in \bar{\Omega},$$

with the corresponding function values

$$f_{i,j} = f(\xi_{i,j}, \phi_j),$$

and we introduce the change of variable from $\bar{\Omega}$ to the disk E in (3.1)

$$(4.1) \qquad S(\xi, \phi) = \left(\frac{2\xi}{\rho(\phi)}, \phi \right) = \Big(S_1(\xi,\phi), S_2(\xi,\phi) \Big) := (r, \theta).$$

By this way we can interpolate on E using the data of the function on the grid on $\bar{\Omega}$ by the function

$$(4.2) \quad \mathcal{I}[f](S(\xi,\phi)) = \frac{\sum_{i=0}^{n_1} {}'' \sum_{j=0}^{n_2-1} \frac{(-1)^{i+j}}{S_1(\xi,\phi)-S_1(\xi_{i,j},\phi_j)} \operatorname{cst}\left(\frac{S_2(\xi,\phi)-S_2(\xi_{i,j},\phi_j)}{2} \right) f_{i,j}}{\sum_{i=0}^{n_1} {}'' \sum_{j=0}^{n_2-1} \frac{(-1)^{i+j}}{S_1(\xi,\phi)-S_1(\xi_{i,j},\phi_j)} \operatorname{cst}\left(\frac{S_2(\xi,\phi)-S_2(\xi_{i,j},\phi_j)}{2} \right)}.$$

This is similar to a technique introduced by De Marchi et al. [9, 16, 17] called the fake nodes (or mapped basis) approach, which consists in considering the interpolant constructed on the mapped interpolation nodes and a set of evaluation points, mapped as well.

The interpolant (4.2) inherits several nice properties from the interpolant (3.2).

PROPOSITION 4.2. *Let S be as in (4.1). Then the Lebesgue constant $\bar{\Lambda}_{n_1 n_2}$ of the interpolant (4.2) at the set of nodes $G_{i,j}$ satisfies*

$$\bar{\Lambda}_{n_1 n_2} = \mathcal{O}(\log n_1 \log n_2).$$

Proof. By definition, the Lebesgue constant of (4.2) is

$$\bar{\Lambda}_{n_1 n_2} = \max_{(\xi,\phi)\in\bar{\Omega}} \sum_{i_j=0}^{n_1(n_2-1)} |B_{i_j}(S(\xi,\phi))| = \max_{(r,\theta)\in S(\bar{\Omega})\equiv E} \sum_{i_j=0}^{n_1(n_2-1)} |B_{i_j}(r,\theta)| = \Lambda_{n_1 n_2},$$

where $\Lambda_{n_1 n_2}$ is the Lebesgue constant of the interpolant (3.2). Theorem 3.1 then yields the result. □

Note that this is true in particular when the points $G_{i,j}$ are such that their images under the map S are conformally shifted nodes in the disk.

5. Convergence. In order to study its convergence in a starlike domain, we first consider the interpolant in the disk (or the rectangle). Then, we can prove the following bound:

THEOREM 5.1. *Let $f \in \mathcal{C}^\infty(B)$ be such that for any fixed r the function $f(r, \cdot)$ satisfies the hypothesis of Theorem 2.5 and for any fixed θ the function $f(\cdot, \theta)$ satisfies the hypothesis of Theorem 2.2. Then the error of the interpolant (3.2) can be bounded as*

(5.1)
$$\|f - \mathcal{I}[f]\| \le \left(2 \min \left\{ \Lambda_{n_1}^{(1)}, \Lambda_{n_2}^{(2)} \right\} + \Lambda_{n_1}^{(1)} \Lambda_{n_2}^{(2)} + 1 \right)$$
$$\times \max \left\{ \frac{4 M_1}{\sigma - 1} \sigma^{-n_1}, 2 M_2 \operatorname{ctg} \left(\frac{a}{2} \right) e^{-a n_2} \right\}.$$

Proof. First, let us consider the points $(\bar{r}, \bar{\theta}) \in B$ such that

$$(\bar{r}, \bar{\theta}) = \arg \max_{(r, \theta) \in B} |f(r, \theta) - \mathcal{I}[f](r, \theta)|.$$

Then, with the notations

$$\mathcal{I}_1[f](r, \theta) := \sum_{i=0}^{n_1} b_i^{(1)}(r) f(r_i, \theta) \qquad \text{and} \qquad \mathcal{I}_2[f](r, \theta) := \sum_{j=0}^{n_2 - 1} b_j^{(2)}(\theta) f(r, \theta_j),$$

we can compute

$$\|f - \mathcal{I}[f]\| = \left| f(\bar{r}, \bar{\theta}) - \mathcal{I}[f](\bar{r}, \bar{\theta}) \right| = \left| f(\bar{r}, \bar{\theta}) - \mathcal{I}_1[\mathcal{I}_2[f]](\bar{r}, \bar{\theta}) \right|$$
$$= \left| f(\bar{r}, \bar{\theta}) - \mathcal{I}_1[f](\bar{r}, \bar{\theta}) + \mathcal{I}_1[f](\bar{r}, \bar{\theta}) - \mathcal{I}_1[\mathcal{I}_2[f]](\bar{r}, \bar{\theta}) \right|$$
$$\le \left| f(\bar{r}, \bar{\theta}) - \mathcal{I}_1[f](\bar{r}, \bar{\theta}) \right| + \left| \mathcal{I}_1[f](\bar{r}, \bar{\theta}) - \mathcal{I}_1[\mathcal{I}_2[f]](\bar{r}, \bar{\theta}) \right|$$
$$= \left| f(\bar{r}, \bar{\theta}) - \mathcal{I}_1[f](\bar{r}, \bar{\theta}) \right| + \left| \mathcal{I}_1 \left[f(\cdot, \bar{\theta}) - \mathcal{I}_2[f](\cdot, \bar{\theta}) \right](\bar{r}) \right|,$$

where the last line holds in view of the linearity of $\mathcal{I}_1$. Thus,

$$\|f - \mathcal{I}[f]\| \le \left| f(\bar{r}, \bar{\theta}) - \mathcal{I}_1[f](\bar{r}, \bar{\theta}) \right| + \|\mathcal{I}_1\| \left| f(\bar{r}, \bar{\theta}) - \mathcal{I}_2[f](\bar{r}, \bar{\theta}) \right|$$
$$\le (1 + \Lambda_{n_1}^{(1)}) \frac{4 M_1}{\sigma - 1} \sigma^{-n_1} + \Lambda_{n_1}^{(1)} (1 + \Lambda_{n_2}^{(2)}) 2 M_2 \operatorname{ctg} \left(\frac{a}{2} \right) e^{-a n_2}.$$

Here we have used the classic estimate for interpolation [24, p. 24]

$$\|h - p_n[h]\| \le (1 + \Lambda_n) \|h - p^*\|,$$

with p^* denoting the best approximation of h in $\mathbb{P}_n$, and the fact that, since $\mathcal{I}_1$ (respectively $\mathcal{I}_2$) corresponds to the interpolation at Chebyshev nodes of the second kind (respectively trigonometric interpolation at equidistant nodes), we have from Theorem 2.2 that

$$\|h - p^*\| \le \|h - \mathcal{I}_1[h]\| \le \frac{4 M_1}{\sigma - 1} \sigma^{-n_1},$$

for a function $h : \mathbb{R} \to \mathbb{R}$ analytic in the ellipse $\mathcal{E}_\sigma$ and similarly for $\mathcal{I}_2$ with Theorem 2.5. Therefore, we have

$$\|f - \mathcal{I}[f]\| \leq \left(2\Lambda_{n_1}^{(1)} + \Lambda_{n_1}^{(1)}\Lambda_{n_2}^{(2)} + 1\right) \max\left\{\frac{4M_1}{\sigma - 1}\sigma^{-n_1}, 2M_2 \operatorname{ctg}\left(\frac{a}{2}\right)e^{-an_2}\right\},$$

and since we can repeat the same reasoning by exchanging $\mathcal{I}_1$ with $\mathcal{I}_2$ and vice versa we obtain (5.1).   □

Similarly we can prove a convergence theorem with weaker conditions by proceeding as in the proof of Theorem 5.1.

THEOREM 5.2. *Let f be a function such that for any fixed r the function $f(r, \cdot)$ satisfies the hypotheses of Theorem 2.4 and for any fixed θ the function $f(\cdot, \theta)$ satisfies the hypotheses of Theorem 2.1. Then the error of the interpolant (3.2) can be bounded as*

$$\|f - \mathcal{I}[f]\| \leq \left(2\min\left\{\Lambda_{n_1}^{(1)}, \Lambda_{n_2}^{(2)}\right\} + \Lambda_{n_1}^{(1)}\Lambda_{n_2}^{(2)} + 1\right)\max\left\{\frac{4V_1}{\pi\nu(n-\nu)^\nu}, \frac{V_2}{\pi n^\mu}\left(\frac{1}{n} + \frac{2}{\mu}\right)\right\}.$$

Furthermore, we obtain similar bounds for the interpolant at conformally shifted nodes by following the proof of Theorem 5.1 but estimating with the best approximation in the spaces $\mathcal{R}_{n_1}$ and Σ_{n_2} introduced in Section 3 instead of the best approximation in the polynomial spaces.

THEOREM 5.3. *Let $f \in \mathcal{C}^\infty(B)$ be such that for any fixed r the function $f(r, \cdot)$ satisfies the hypotheses of Theorem 2.6 and for any fixed θ the function $f(\cdot, \theta)$ satisfies the hypotheses of Theorem 2.3. Then, we can bound the error of the interpolant (3.3) as*

$$\|f - \mathcal{I}[f]\| \leq \left(2\min\left\{\Lambda_{n_1}^{(1)}, \Lambda_{n_2}^{(2)}\right\} + \Lambda_{n_1}^{(1)}\Lambda_{n_2}^{(2)} + 1\right)\max\left\{C_1\sigma^{-n_1}, C_2 e^{-an_2}\right\},$$

for two constants C_1, C_2, where C_1 depends on σ and g_1, C_2 on a and g_2, and both on the function f.

Finally, note that the interpolant in the starlike domain inherits the error from the interpolant on the disk.

THEOREM 5.4. *Let S be as in (4.1), $\mathcal{I}$ as in (3.2) (or (3.3)), and $\mathcal{I}^S$ as in (4.2). Then, for a function $f : \Omega \to \mathbb{R}$ we have*

$$\left\|f - \mathcal{I}^S[f]\right\|_\Omega = \|h - \mathcal{I}[h]\|_E,$$

where $h = f \circ S^{-1}$.

Proof. By definition we have $\mathcal{I}^S = \mathcal{I} \circ S$. Then, if we consider as h the function such that $h \circ S = f$, we have

$$\left\|\mathcal{I}^S[f] - f\right\|_\Omega = \|\mathcal{I} \circ S - h \circ S\|_\Omega = \|\mathcal{I}[h] - h\|_{S(\Omega)},$$

and $S(\Omega) = E$.   □

Consequently, since the interpolant converges as that of the function $h = f \circ S^{-1}$, where

$$S^{-1}(r, \theta) := \left(\frac{r\rho(\theta)}{2}, \theta\right),$$

the convergence depends on f and S; a smoother function ρ will lead to a better interpolant (4.2) of the function f in $\bar{\Omega}$.

TABLE 6.1
Rectangles for the evaluation points with the various domains.

	Rectangle
ρ_1	$[-1, 3] \times [-2, 2]$
ρ_2	$[-2, 2] \times [-2, 2]$
ρ_3	$[-13, 13] \times [-10, 10]$
ρ_4	$[-4, 4] \times [-4, 4]$
ρ_5	$[-2, 2] \times [-2, 2]$

We have also interpolated on non-smooth domains but the results were not satisfactory as the function h itself is non-smooth along the boundary, i.e., for $r = 2$. A way of dealing with such a non-smooth function ρ, as for example the polar representation of the square

$$(5.2) \qquad \rho(\theta) = \min \left\{ \frac{1}{|\cos(\theta)|}, \frac{1}{|\sin(\theta)|} \right\},$$

is to replace it with a close enough smoother approximant $\widetilde{\rho}$ and interpolate in the approximate domain $\widetilde{\Omega} = \widetilde{S}(E)$ instead of $\bar{\Omega} = S(E)$, where $\widetilde{S}$ is the function S with $\widetilde{\rho}$ in place of ρ. Some tests in this direction are reported in the next section.

6. Numerical tests. In this section we test the interpolant (4.2) on domains inside the curve

$$z(\theta) := \Big(\rho(\theta) \cos(\theta), \rho(\theta) \sin(\theta) \Big)$$

for a 2π-periodic boundary parametrization

$$\rho(\theta) : [0, 2\pi] \to \mathbb{R}^{>0}.$$

We first consider the following domains (see Figure 6.1):
- The limaçon

$$\rho_1(\theta) = 1.5 + 1.2 \cos(\theta).$$

- A first butterfly-shaped domain

$$\rho_2(\theta) = 1 - \cos(\theta) \sin(3\theta).$$

- A second butterfly-shaped domain

$$\rho_3(\theta) = 7.5 - \sin(\theta) + 4\sin(3\theta) - \sin(7\theta) + 3\cos(2\theta).$$

- The asterisk

$$\rho_4(\theta) = \sin(10\,\theta) + 2.2.$$

To estimate the error, we consider a grid of 170×170 uniformly-spaced points in a rectangle around the domain (see Table 6.1 for the rectangles), and we filter them by considering only the points inside the domain. Then, we compute the maximum of the absolute value of the difference between the interpolant and the function in these points.

Notice that all these domains are constructed via a smooth function ρ. Thus, the expected convergence behaviour will not be influenced by infinitely smooth changes of variable such as conformal point shifts.
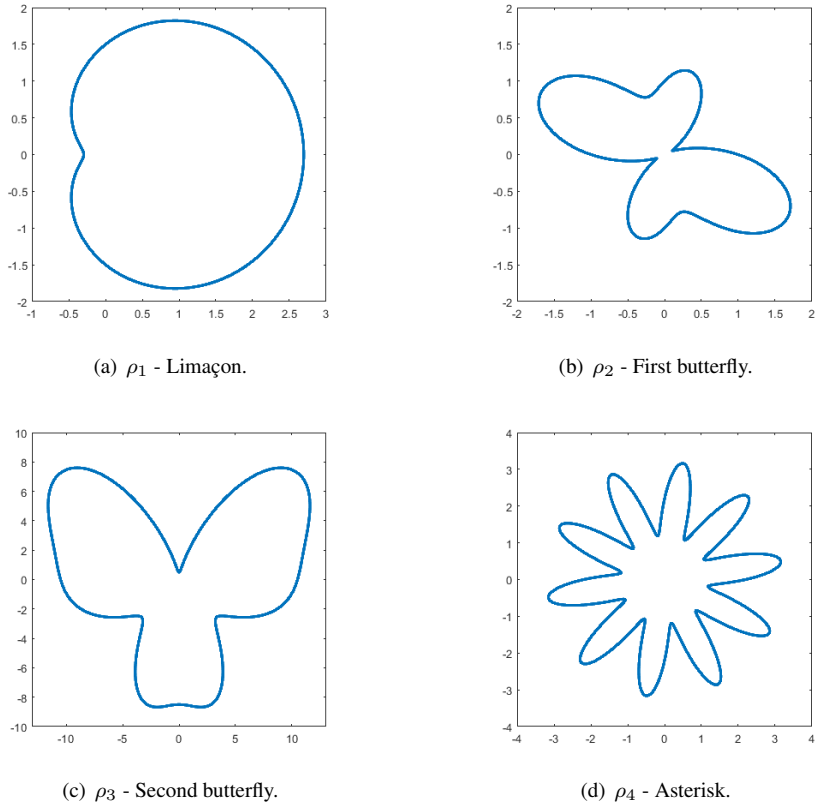
(a) ρ_1 - Limaçon.

(b) ρ_2 - First butterfly.

(c) ρ_3 - Second butterfly.

(d) ρ_4 - Asterisk.

FIG. 6.1. *Test domains.*

TABLE 6.2
Errors with the function f_1 in the various domains.

(n_1, n_2)	ρ_1	ρ_2	ρ_3	ρ_4
(10,30)	1.6762e–02	1.3439e–01	1.4178e+01	2.8832e+01
(20,60)	1.6080e–07	3.3468e–04	2.1093e+00	3.0920e+00
(40,120)	8.5265e–14	1.3499e–10	9.0279e–02	1.5704e–02
(80,240)	1.2790e–13	7.1054e–14	2.0515e–05	4.6051e–07
(160,480)	1.4921e–13	1.0303e–13	9.9476e–14	5.6843e–13

We document our computations with two infinitely smooth functions: a first one which does not require point shifts

$$f_1(x, y) = 3e^{-x^2 + y + 1} + 3$$

(on the left in Figure 6.2) and for which we expect (approximate) exponential convergence. As we observe in Table 6.2, each error is approximately the square of that on the previous row when (n_1, n_2) is doubled; this indeed reflects an exponential decay of the error.

To take advantage of the ability of linear barycentric rational interpolation to accommodate steep gradients (fronts) by simply replacing the nodes in the "classical" interpolant with shifted ones which accumulate in the vicinity of the fronts, i.e., $f_{ij} := f(g_1(r_i)\rho(g_2(\theta_j)), g_2(\theta_j))$,
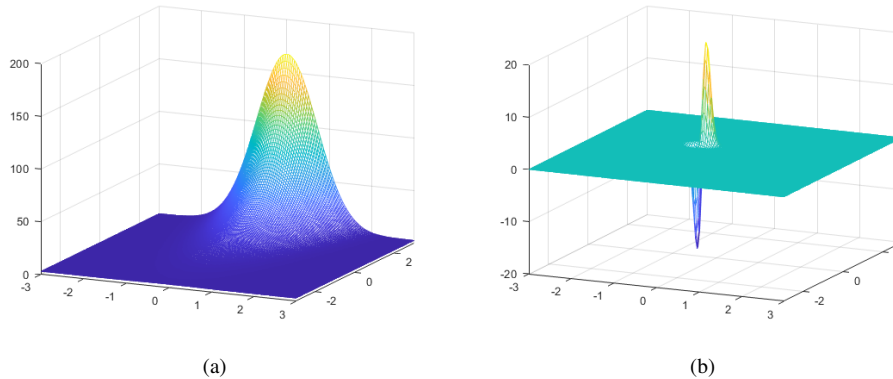
(a)   (b)

FIG. 6.2. *On the left, the first test function f_1, and on the right, the second test function f_2 with the parameters used in the computations.*

TABLE 6.3
Errors with the function f_2 for the first two domains.

(n_1, n_2)	ρ_1	ρ_1 conf	ρ_2	ρ_2 conf
(10,30)	2.2524e+01	4.9054e+00	1.7898e+01	1.8408e+00
(20,60)	7.7530e+00	1.7487e–02	4.6606e+00	3.7443e–02
(40,120)	1.0473e–01	6.2046e–07	6.1903e–02	1.0631e–05
(80,240)	2.2811e–07	1.8474e–13	1.5352e–06	5.8037e–13

we use the interpolant $\mathcal{I}[f]$ in (4.2), and we consider secondly a function (on the right in Figure 6.2) with a front in a precise location, i.e.,

$$f_2(x,y) = 40 \frac{\mathrm{erf}\left(\sqrt{\epsilon/2}(x+0.6)\right)}{\mathrm{erf}(\sqrt{\epsilon/2})} e^{-30(x+0.6)^2} e^{-60(y-0.6)^2},$$

where $\epsilon = 100$ and erf is the error function; f_2 has a front in $(-0.6, 0.6)$ (which becomes $(0.6\sqrt{2}, \frac{7\pi}{4})$ in polar coordinates). We use the conformal maps

$$g_1 = \beta + \frac{1}{\alpha}\tan\left(\lambda(x-\mu)\right) \quad \text{and} \quad g_2(\theta) = -i\log\left(\frac{e^{i\phi} + \eta e^{i\theta}}{1 + e^{i\phi}\eta e^{-i\theta}}\right)$$

with β and ϕ such that the nodes cluster around the location of the front and for the density $\alpha = 2.8$ for g_1 and $\eta = 0.65$ for g_2. g_1 and g_2 are, respectively, the Bayliss-Turkel map [5] and the map introduced by the authors in [10]. (Since everything is smooth, the error is horizontal at the optimal values, and the results are not very sensitive to the parameters there; see the second column of the tables in [12].) The results, displayed in Tables 6.3 and 6.4, indeed show that, as in the uni-dimensional case, we achieve a much faster convergence by using conformal maps to cluster nodes in the vicinity of the location of a front instead of the plain Chebyshev and equispaced points.

Furthermore, we consider a domain which corresponds to a non-smooth ρ, the square $[-1, 1]^2$, parametrized by the function (5.2) which we denote by ρ_5. In this case, approximating functions with the transplanted interpolant often leads to catastrophic results; see the columns ρ_5 in Table 6.5. To avoid this, we slightly modify the domain by approximating ρ_5 with a

TABLE 6.4
Errors with the function f_2 for the next two domains.

(n_1, n_2)	ρ_3	ρ_3 conf	ρ_4	ρ_4 conf
(10,30)	1.8077e+01	1.3739e+01	2.2392e+01	1.3262e+01
(20,60)	7.6290e+00	2.7313e+00	2.1117e+01	5.3838e+00
(40,120)	1.3786e+00	2.6799e–02	1.1580e+01	7.5581e–01
(80,240)	1.9880e–02	1.3075e–06	9.3368e–01	7.3685e–03
(160,480)	2.3293e–08	1.0303e–13	1.5659e–03	1.3545e–08

TABLE 6.5
Errors with ρ_5 and its approximation $\widetilde{\rho_5}$.

(n_1, n_2)	f_1		f_2		
	ρ_5	$\widetilde{\rho_5}$	ρ_5	$\widetilde{\rho_5}$	$\widetilde{\rho_5}$ conf
(10,30)	2.9917e+00	4.4789e–01	9.3838e+03	1.2996e+01	1.8835e+00
(20,60)	3.1510e+00	2.6646e–01	1.5954e+09	7.4563e+00	1.3315e+00
(40,120)	Inf	7.7975e–02	Inf	1.9865e+00	1.0297e–01
(80,240)	Inf	3.7900e–02	Inf	4.9346e–01	4.0428e–02
(160,480)	Inf	4.8907e–03	Inf	2.1970e–01	8.1943e–03

smooth interpolant $\widetilde{\rho_5}$, and we use the interpolant transplanted via the function

$$\tilde{S}(\xi, \phi) = \left(\frac{2\xi}{\widetilde{\rho_5}(\phi)}, \phi \right) = \left(\widetilde{S}_1(\xi, \phi), \widetilde{S}_2(\xi, \phi) \right) := (r, \theta).$$

For Table 6.5 we approximate ρ_5 via the approximant produced by the AAA algorithm [23]: the corresponding $\widetilde{\rho_5}$ clearly gives a better interpolant than ρ_5. Unfortunately, because of its "almost corner", the AAA approximant may lead, in practice, to an interpolant with a slower than exponential convergence in the neighbourhood of the corners. Furthermore, the interpolant is obtained merely in an approximation of the original domain $[-1, 1]^2$.

As a last test, we consider a sketch of Switzerland, whose boundary we simplify in order to have a domain which is starlike with respect to the origin (see Figure 6.3). To obtain the boundary curve, we extracted some points which we use as nodes to interpolate the unknown ρ_6 representing the boundary of the "Swiss-like" domain. Then we approximate the curve with Berrut's first interpolant R_0 (see, e.g., [6, 21]), which produces an approximation—let us denote it by $\widetilde{\rho_6}$—of the unknown ρ_6 (see Figure 6.4). In this case, the rectangle in which we compute the error of the interpolant is $[-2.5, 1.5] \times [-2, 1.5]$. In Table 6.6 we display the errors produced with the functions f_1 and f_2. The exponential convergence does not yet show up without conformal shift but it does with such a shift.

7. Concluding remarks. The present work has introduced a simple generalisation of linear barycentric rational interpolants to two-dimensional domains. The idea is to parameterize a (starlike) domain with polar coordinates and to use linear barycentric interpolation in the radial direction and its trigonometric version in the circular (homothetic) direction. (In reality, the interpolation happens in a disk to which the original problem is transplanted.) Up to a logarithmic factor (which arises from the proof but may not appear in practice), the resulting tensor-product-like interpolant converges exponentially when the function is analytic and with the order of $\mathcal{O}(h^\nu)$ when $f^{(\nu)}$ has bounded variation. Impressive numerical examples amply confirm these theoretical convergence results.

We do not want to conceal certain limitations of the method. The most important one seems to be the fact that the rapid convergence requires that the boundary parametrization
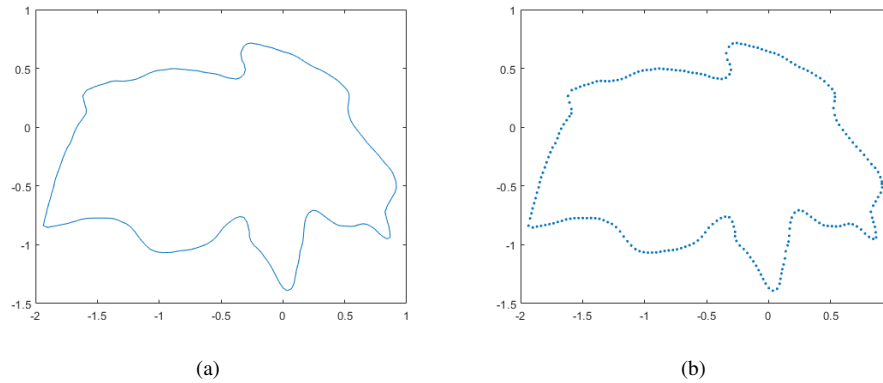
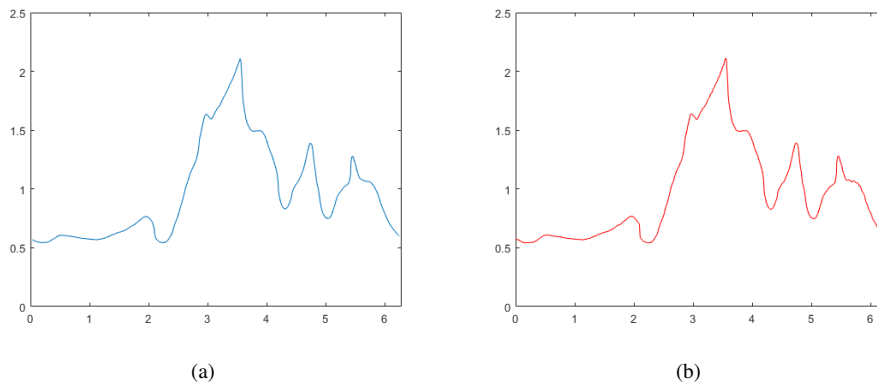FIG. 6.3. *Swiss-like domain: (a) the sketch; (b) the extracted nodes.*

FIG. 6.4. *(a) ρ_6; (b) the approximation $\widetilde{\rho}_6$.*

is as smooth as the interpolated function f, as the interpolant involves the trigonometric interpolation of f along the boundary. Another one is the fact that the boundary curve cannot be arbitrary: for instance, its interior must contain a point to be chosen as the center of the domain from which the representation of the curve does not have too large derivative.

One can easily generalize the method to accomodate functions with several fronts by the method introduced in [13] and extended to the circular case in [10]. But the required computing power could rapidly approach the limitations of MATLAB on a personal computer.

Another issue is that the point shifts deplete the grid close to the boundary (if the steep fronts are not there). In case f has a disturbing steep gradient outside Ω, one can ensure that a radius passes through the corresponding abscissa and attach poles to the radial interpolant, symmetrically with respect to the radius. That way one may expect to gain about 2–3 digits [13]; the barycentric representation is ideal for this attachment.

Finally, we note that one nice feature of this interpolant is the simplicity of the formulae for its partial derivatives along the lines making up its grid: in radial direction they are given by Schneider and Werner's formula [26], and for the circular direction one finds them in [3] (up to inner derivatives of the variable transformation in the chain rule). These formulae could be used to approach the (infinitely smooth) solutions of partial differential equations such

TABLE 6.6
Errors for the "Swiss-like" domain.

(n_1, n_2)	f_1 $\widetilde{\rho}_6$	f_2 $\widetilde{\rho}_6$	$\widetilde{\rho}_6$ conf
(40,120)	4.3451e–01	9.6853e+00	5.3945e+00
(80,240)	3.2449e–01	9.2768e+00	6.3695e–01
(160,480)	1.5968e–01	6.2080e+00	3.0078e–01
(320,960)	4.1611e–02	1.3068e+00	2.6339e–02
(640,1920)	1.9271e–02	4.1124e–01	8.5433e–05
(1280,3840)	1.7645e–03	5.4788e–02	1.0787e–09

as Poisson problems in starlike domains. However, the fact that the mesh is not orthogonal will lead to more complicated formulae for the Laplacian (chain rule) than just those of Schneider-Werner and Baltensperger.

REFERENCES

[1] J. ABOUIR AND A. CUYT, *Error formulas for multivariate rational interpolation and Padé approximation*, J. Comput. Appl. Math., 31 (1990), pp. 233–241.

[2] A. P. AUSTIN, M. KRISHNAMOORTHY, S. LEYFFER, S. MRENNA, J. MÜLLER, AND H. SCHULZ, *Multivariate rational approximation*, Preprint on arXiv, 2019. https://arxiv.org/abs/1912.02272

[3] R. BALTENSPERGER, *Some results on linear rational trigonometric interpolation*, Comput. Math. Appl., 43 (2002), pp. 737–746.

[4] R. BALTENSPERGER, J.-P. BERRUT, AND B. NOËL, *Exponential convergence of a linear rational interpolant between transformed Chebyshev points*, Math. Comp., 68 (1999), pp. 1109–1120.

[5] A. BAYLISS AND E. TURKEL, *Mappings and accuracy for Chebyshev pseudo-spectral approximations*, J. Comput. Phys., 101 (1992), pp. 349–359.

[6] J.-P. BERRUT, *Rational functions for guaranteed and experimentally well-conditioned global interpolation*, Comput. Math. Appl., 15 (1988), pp. 1–16.

[7] ———, *The conditioning of a linear barycentric rational interpolant*, in Realization and Model Reduction of Dynamical Systems, C. Beattie, P. Benner, M. Embree, S. Gugercin, and S. Lefteriu, eds., Springer, Cham, 2022, pp. 23–37.

[8] J.-P. BERRUT, R. BALTENSPERGER, AND H. D. MITTELMANN, *Recent developments in barycentric rational interpolation*, in Trends and Applications in Constructive Approximation, D. H. Mache, J. Szabados, M. G. Bruin, eds., vol. 151 of Internat. Ser. Numer. Math., Birkhäuser, Basel, 2005, pp. 27–51.

[9] J.-P. BERRUT, S. DE MARCHI, G. ELEFANTE, AND F. MARCHETTI, *Treating the Gibbs phenomenon in barycentric rational interpolation and approximation via the S-Gibbs algorithm*, Appl. Math. Lett., 103 (2020), Art. 106196, 7 pages.

[10] J.-P. BERRUT AND G. ELEFANTE, *A periodic map for linear barycentric rational trigonometric interpolation*, Appl. Math. Comput., 371 (2020), Art. 124924, 8 pages.

[11] ———, *Bounding the Lebesgue constant for a barycentric rational trigonometric interpolant at periodic well-spaced nodes*, J. Comput. Appl. Math., 398 (2021), Art. 113664, 11 pages.

[12] J.-P. BERRUT AND H. D. MITTELMANN, *Point shifts in rational interpolation with optimized denominator*, in Proceedings of the 2001 International Symposium on Algorithms for Approximation IV, J. Levesley, I. J. Anderson and J. C. Mason, eds, University of Huddersfield, Huddersfield, 2002, pp. 420–427.

[13] ———, *Adaptive point shifts in rational approximation with optimized denominator*, J. Comput. Appl. Math., 164/165 (2004), pp. 81–92.

[14] V. I. BURENKOV, *Sobolev Spaces on Domains*, Teubner, Stuttgart, 1998.

[15] A. A. M. CUYT AND B. M. VERDONK, *Multivariate rational interpolation*, Computing, 34 (1985), pp. 41–61.

[16] S. DE MARCHI, F. MARCHETTI, E. PERRACCHIONE, AND D. POGGIALI, *Polynomial interpolation via mapped bases without resampling*, J. Comput. Appl. Math., 364 (2020), Art. 112347, 12 pages.

[17] ———, *Multivariate approximation at fake nodes*, Appl. Math. Comput., 391 (2021), Art. 125628, 17 pages.

[18] R. A. DEVORE AND X. M. YU, *Multivariate rational approximation*, Trans. Amer. Math. Soc., 293 (1986), pp. 161–169.

[19] D. GAIER, *Ableitungsfreie Abschätzungen bei trigonometrischer Interpolation und Konjugierten-Bestimmung*, Computing (Arch. Elektron. Rechnen), 12 (1974), pp. 145–148.

[20] P. HENRICI, *Essentials of Numerical Analysis with Pocket Calculator Demonstrations*, Wiley, New York, 1982.

[21] K. HORMANN, *Barycentric interpolation*, in Approximation Theory XIV, G. E. Fasshauer and L. L. Schumaker, eds., vol. 83 of Springer Proc. Math. Stat., Springer, Cham, 2014, pp. 197–218.

[22] B. N. KHOROMSKIJ, *Tensor Numerical Methods in Scientific Computing*, De Gruyter, Berlin, 2018.

[23] Y. NAKATSUKASA, O. SÈTE, AND L. N. TREFETHEN, *The AAA algorithm for rational approximation*, SIAM J. Sci. Comput., 40 (2018), pp. A1494–A1522.

[24] M. J. D. POWELL, *Approximation Theory and Methods*, Cambridge University Press, Cambridge, 1981.

[25] T. RIVLIN, *The Chebyshev Polynomials*, Wiley, New York, 1974.

[26] C. SCHNEIDER AND W. WERNER, *Some new aspects of rational interpolation*, Math. Comp., 47 (1986), pp. 285–299.

[27] L. SCHUMAKER, *Spline Functions*, SIAM, Philadelphia, 2015.

[28] P. SESHADRI, P. CONSTANTINE, P. GONNET, AND G. T. PARKS, *Sparse robust rational interpolation for parameter-dependent aerospace models*, in 54 AIAA/ASME/ASCE/AHS/ASC Structures, Structural Dynamcis and Material Conference, American Institute of Aeronautics and Astronautics, Reston, 2013, Art. AIAA 2013-1680.

[29] L. N. TREFETHEN, *Approximation Theory and Approximation Practice*, SIAM, Philadelphia, 2013.

[30] G. B. WRIGHT, M. JAVED, H. MONTANELLI, AND L. N. TREFETHEN, *Extension of Chebfun to periodic functions*, SIAM J. Sci. Comput., 37 (2015), pp. C554–C573.